

# In vivo evaluation of doxorubicin carried with long circulating and remote loading proliposome

Wang Junping, Yoshie Maitani\*, Kozo Takayama, Tsuneji Nagai

*Department of Pharmaceutics, Hoshi University, Ebara 2-4-41, Shinagawa-ku, Tokyo 142-8501, Japan*

Received 27 November 1999; received in revised form 21 February 2000; accepted 13 March 2000

## Abstract

Long circulating and remote loading proliposome (LRP-L) was a kind of transparent solution and composed of soybean phosphatidylcholine (SPC), cholesterol, polyethylene glycol derivative of distearoylphosphatidyl ethanolamine (PEG-DSPE) and oleic acid sodium salt. When LRP-L was mixed with 0.9% NaCl aqueous solution containing doxorubicin (DXR), liposomes formed and automatically loaded DXR, in which sonication and extruders were not needed. The average diameter of the liposomal DXR in saline was  $129.0 \pm 1.9$  nm and the encapsulation efficiency was  $98.1 \pm 0.6\%$ . The pharmacokinetics, biodistribution, acute toxicity and anticancer effect of DXR carried with LRP-L (LRP-L-DXR) were studied. The plasma concentration–time curves of DXR were best fitted to the triexponential decay curves. The area under the plasma concentration–time curve (AUC) of LRP-L-DXR was 22 and five times of free DXR (F-DXR) and conventional cardiolipin liposomal DXR (CL-DXR), respectively. Following i.v. administration, the biodistribution of LRP-L-DXR in the heart and the liver, unlike that of CL-DXR, was not greater than that of F-DXR. However, the biodistribution of LRP-L-DXR in the spleen was less than that of CL-DXR and greater than that of F-DXR. The acute toxicity of LRP-L-DXR was decreased compared with that of F-DXR. The anticancer effect of LRP-L-DXR was significantly increased compared with that of F-DXR in the ascitic M5076 tumor model of C57BL/6 mice and had no significant difference compared with that of doxorubicin HCl liposome injection (Doxil). © 2000 Elsevier Science B.V. All rights reserved.

*Keywords:* Proliposome; Long circulation; Remote loading; Doxorubicin; Pharmacokinetics; Biodistribution; Anticancer action

## 1. Introduction

Proliposome was introduced into liposome technology more than 10 years ago to overcome some disadvantages of the liposome drug delivery

system (Paney et al., 1986a). When proliposome is mixed with a water phase containing drug before use, liposomes form automatically and load the drug. It has been reported that proliposome was used to carry amphotericin B (Paney et al., 1986b), indomethacin (Katare et al., 1991a), non-steroidal anti-inflammatory analogues (Katare et al., 1991b) and doxorubicin (DXR) (Wang et al., 1994; Lee et al., 1996). DXR is one of the most

\* Corresponding author. Tel.: +81-3-54985782; fax: +81-3-54985782.

*E-mail address:* yoshie@hoshi.ac.jp (Y. Maitani).

widely used anticancer agents because of its broad spectrum of anticancer activity, reasonable therapeutic index, and intriguing biological and physicochemical actions. The major problem in cancer chemotherapy with DXR is the toxic responses, among which cardiomyopathy is the most serious. In order to reduce the toxic responses and increase the anticancer effects of DXR, liposomes were selected to carry DXR as early as the late 1970s (Fossen and Tokes, 1979).

The main problems of proliposome can be described as follows: (1) the particle size distribution could not be controlled within a suitable range between 100–200 nm; (2) the encapsulation efficiency was low; (3). The circulation time in the blood circulating system was short. Proliposome was prepared by many methods, including crystal-film method, powder thin film method, freezing and drying method and spray drying method. During the past 10 years, much improvement was made in liposome technology, of which long circulation technology and remote loading technology used in Doxil are more important. In Doxil (Working et al., 1994), particle size distribution of DXR liposomes is controlled by extruders, encapsulation efficiency of DXR is increased by transmembrane ammonium sulfate gradient loading method and polyethylene glycol derivative of distearoylphosphatidyl ethanolamine (PEG-DSPE) is used to protect DXR liposomes (Stealth liposomes) circulating in the blood stream.

To simplify the preparation method of Doxil, we combined the long circulation technology, remote loading technology and proliposome technology together and prepared a novel kind of proliposome-long circulating and remote loading proliposome (LRP-L) used as DXR carrier.

The aim of the present study is to evaluate the pharmacokinetics, biodistribution, acute toxicity and anticancer effect of DXR carried by LRP-L (LRP-L-DXR).

## 2. Materials and methods

### 2.1. Materials

Soybean phosphatidylcholine (SPC) was kindly

supplied by Fuda Pharmaceutical (Shanghai, China). Cholesterol was purchased from Sigma (St Louis, MO). Polyethylene glycol derivative of distearoylphosphatidyl ethanolamine (PEG-DSPE, mean molecular weight of PEG: 2000) was kindly supplied by NOF Co. Ltd. (Tokyo, Japan), oleic acid sodium salt was purchased from Tokyo Kasei Kogyo (Tokyo, Japan). DXR HCl was supplied by Kyowa Hakkō Kogyo, Japan. Doxorubicin HCl liposome injection (Doxil) was kindly supplied by SEQUUS Pharmaceuticals, Inc. (Menlo Park, CA). All solvents used for chromatographic determination of DXR were of HPLC grade. All other reagents and solvents were of analytical grade.

The animals used were 18–20 g male C57BL/6 mice and were supplied by Tokyo Animal Experiment Center (Tokyo, Japan). All mice used in the study were raised and kept in SPF animal laboratory. The murine histiocytoma M5076 tumor cells were supplied by the Cancer Chemotherapy Center of Japanese Foundation for Cancer Research (Tokyo, Japan). After four transplant generations of ascitic M5076, the tumor cells were used in this study.

### 2.2. Liposome preparation and DXR encapsulation

Preparation of LRP-L was based upon the ethanol injection method (Batzri and Korn, 1973). The required amounts of SPC, cholesterol, PEG-DSPE and oleic acid sodium salt were dissolved in mixed solvent of ethanol:glycerin (3:1), sterilized by filtration, filled into ampules (2 ml/ampule) and sealed after oxygen was driven out with aseptic nitrogen gas. Each ampule contained 200 mg SPC, 40 mg PEG-DSPE, 15 mg cholesterol, 30 mg oleic acid sodium salt and was used to carry 30 mg DXR. The whole preparation procedure was carried out in clean bench and all materials were pyrogen-free and sterilized. When LRP-L was injected into 0.9% NaCl aqueous solution containing DXR HCl, liposomes formed and automatically loaded DXR.

Cardiolipin liposomal DXR (CL-DXR) was prepared using the previously reported method (Rahman et al., 1985). Briefly, 5.6  $\mu\text{mole}$  cardiolipin (Sigma, St Louis, MO) was complexed to 11.2  $\mu\text{mole}$  DXR in methanol solution and the mixture was then evaporated to dryness under  $\text{N}_2$  gas. To this dried mixture, 28.5  $\mu\text{mole}$  SPC, 19.5  $\mu\text{mole}$  cholesterol and 11.1  $\mu\text{mole}$  stearylamine (Sigma, St Louis, MO) were then added in chloroform solution. The mixture was evaporated to dryness under  $\text{N}_2$  gas. The dried lipids were resuspended in 6 ml of 0.01 M phosphate buffer containing 0.85% NaCl (pH 7.4) and sonicated in ice water 10 min three times. The free DXR was separated from the liposomal form using the supercentrifugation method.

### 2.3. Characterization of LRP-L-DXR

The particle size distribution and the zeta potential of LRP-L-DXR were determined using a laser light scattering instrument (ELS800, Otsuka Electronics, Japan). The encapsulation efficiency of LRP-L-DXR is the percentage of DXR carried by liposomes and was determined using the Sephadex G-50 column chromatography method. The LRP-L-DXR was separated from the F-DXR when the mobile phase was saline. The concentration of DXR in free or liposomal form was determined using the HPLC method, which is described in Section 2.4.

### 2.4. Pharmacokinetics and biodistribution of LRP-L-DXR

The mice were fasted for 12 h with only water allowed. DXR of different formulations was administered i.v. through the tail vein at a dose of 5 mg DXR/kg. Blood samples were collected following decapitation and immediately centrifuged at 4000 rpm for 10 min. The plasma samples and the tissue samples including heart, liver, lung, spleen and kidney were kept at  $-20^\circ\text{C}$  until analysis. DXR was extracted from the plasma and the tissue using the HPLC method previously reported (Cox et al., 1991). The HPLC system was composed of an LC-10AS pump (Shimadzu, Japan), a SIL-10A autoinjector (Shimadzu,

Japan), a RF-10AXL fluorescence detector (Ex, 470 nm, Em, 585 nm, Shimadzu, Japan) and a YMC-Pack ODS-A,  $150 \times 6.0$  mm, I.D., S-5  $\mu\text{m}$ , 120A column (YMC, Japan). The mobile phase was 1/15 M  $\text{KH}_2\text{PO}_4 \cdot \text{CH}_3\text{CN} = 75:25$  (V/V, pH 4.16, adjusted with  $\text{H}_3\text{PO}_4$ ) and the flow rate was 1.0 ml/min.

The concentration of DXR in each sample was determined using a constructed calibration curve. Data were analyzed using a nonlinear least-squares data fitting program (Yamaoka et al., 1981). The area under the biodistribution curves of DXR of different formulations (AUC) was calculated using the trapezoid method.

### 2.5. Acute toxicity experiment

The mice used were inoculated tumor cells (as many as in the therapeutic experiment) of M5076 and divided by 20 mice per group. Five days after the inoculation of the ascitic  $1 \times 10^6$  M5076 cells i.p., the mice were administered F-DXR and LRP-L-DXR i.v. at different doses. The acute toxicity of F-DXR and LRP-L-DXR were reflected in the survival rates of the mice in each group.

### 2.6. Anticancer experiment

The mice used were inoculated tumor cells of M5076 and divided into ten mice per group. The ascitic tumor cells were removed from normal donor mice under the shortly acting methoxyflurane inhalation anaesthetic state. The tumor cell suspension was diluted three times with saline. Each animal used in this experiment was inoculated with  $1 \times 10^6$  M5076 cells i.p.. The tumor implantation was carried out in the SPF laboratory. Five days after inoculation, the mice were administered LRP-L-DXR, F-DXR, and saline (control) i.v. in a single dose. Two doses were established, 5.6 and 8.3 mg DXR/kg, respectively. The comparison of the anticancer effects of LRP-L-DXR and Doxil was carried out in the same tumor model and administered i.v. at a dose of 8.3 mg/kg. Increase in life span (ILS) was calculated according to the following equation:  $\text{ILS} = (T/C - 1) 100\%$ , where  $T$  and  $C$  are the median

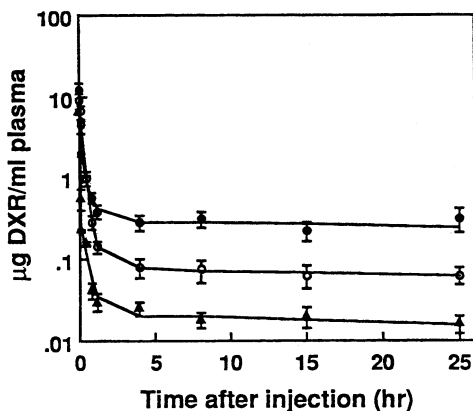


Fig. 1. Plasma concentration–time curves of doxorubicin (DXR) of different formulations following i.v. administration at a dose of 5 mg DXR/kg in C57BL/6 mice. ●, LRP-L-DXR; ○, CL-DXR; ▲, F-DXR. Results are given as means  $\pm$  S.D.,  $n$ , 3.

survival time of the treated mice and the control mice, respectively. ILS was statistically analyzed using the non-parametric Williams–Wilcoxon test.

Table 1  
Pharmacokinetic parameters of F-DXR, CL-DXR and LRP-L-DXR

Parameters <sup>a</sup>	F-DXR	CL-DXR	LRP-L-DXR
CL ( $1 \text{ h}^{-1} \text{ kg}^{-1}$ )	2.2	0.5	0.1
AUC ( $\mu\text{g ml}^{-1} \text{ h}$ )	2.2	10.0	39.7
$V_1$ ( $1 \text{ kg}^{-1}$ )	0.3	0.5	0.3
$V_2$ ( $1 \text{ kg}^{-1}$ )	1.1	0.1	0.5
$V_3$ ( $1 \text{ kg}^{-1}$ )	154.7	39.5	14.6
$V_{ss}$ ( $1 \text{ kg}^{-1}$ )	156.2	40.2	15.4
$T_{1/2} \alpha$ (min)	0.9	8.6	2.0
$T_{1/2} \beta$ (min)	14.9	56.5	17.3
$T_{1/2} \gamma$ (min)	59.5	70.4	70.4
MRT (h)	69.8	80.5	122.3

<sup>a</sup> The following parameters were included, CL, clearance; AUC, area under the plasma–time curve;  $V_1$ ,  $V_2$  and  $V_3$  are the apparent distribution volumes of the first, second and third compartments;  $V_{ss}$ , steady state apparent distribution volume,  $T_{1/2} \alpha$ ,  $T_{1/2} \beta$  and  $T_{1/2} \gamma$  are the half-lives of the  $\alpha$ ,  $\beta$  and  $\gamma$  phases, respectively; MRT is the mean residence time.

### 3. Results

#### 3.1. Characterization of LRP-L-DXR

The average diameter of LRP-L-DXR in saline was  $129.0 \pm 1.9$  nm in 0.9% NaCl ( $n$ , 3). The encapsulation efficiency of LRP-L-DXR in saline was  $98.1 \pm 0.6\%$  ( $n$ , 3). The zeta potential of LRP-L-DXR in saline was  $-13.9 \pm 9.2$  mV ( $n$ , 3).

#### 3.2. Pharmacokinetics and biodistribution of LRP-L-DXR

Plasma clearance of DXR of different formulations following i.v. injection at a single dose of 5 mg DXR/kg through the tail vein of mice is shown in Fig. 1. The plasma concentration–time curves of DXR of different formulations were best fitted to triexponential decay curves.

Pharmacokinetic parameters of DXR of different formulations are shown in Table 1. Table 1 shows that the CL (clearance) and the  $V_{ss}$  (distribution volume at steady state) of LRP-L-DXR were 0.1 and 15.4 ( $1 \text{ kg}^{-1}$ ), while those of F-DXR were 2.2 and 156.2 ( $1 \text{ kg}^{-1}$ ) and those of CL-DXR were 0.5 and 40.2 ( $1 \text{ kg}^{-1}$ ). The AUC of LRP-L-DXR was 39.7 ( $\mu\text{g ml}^{-1} \text{ h}$ ), while those of F-DXR and CL-DXR were 2.2 and 10.0 ( $\mu\text{g ml}^{-1} \text{ h}$ ), respectively. The MRT (mean residence time) of LRP-L-DXR was 122.3 (h), while those of F-DXR and CL-DXR were 69.8 and 80.5 (h), respectively. These findings indicate that LRP-L-DXR circulated for a longer time in the blood circulating system than F-DXR and CL-DXR.

Biodistribution curves of DXR in different formulations are shown in Figs. 2–6. The AUC of the biodistribution curves of DXR of different formulations is shown in Table 2. Fig. 2 shows that when the CL-DXR was administered i.v., less DXR was taken up by the heart tissue than that of F-DXR (0–10 h), but 24 h later the DXR content in the heart tissue was higher than that of F-DXR. Unlike the CL-DXR, following the injection of LRP-L-DXR, DXR taken up by the heart was not more than that of F-DXR. The AUC values of F-DXR, CL-DXR and LRP-L-DXR in the heart were 36.05, 58.72 and 28.92 ( $\text{h } \mu\text{g/g}$ ), respectively (Table 2).

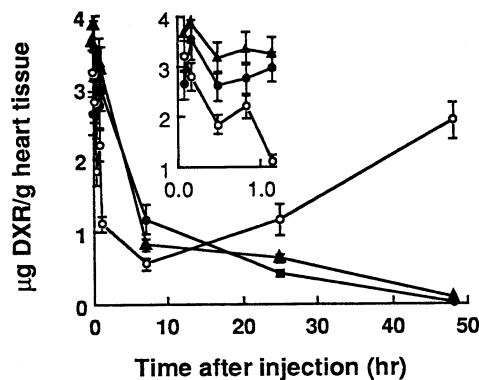


Fig. 2. Drug levels in heart tissue after i.v. injection of doxorubicin (DXR) of different formulations into C57BL/6 mice at a dose of 5 mg DXR/kg.  $\blacktriangle$ , LRP-L-DXR;  $\circ$ , CL-DXR;  $\triangle$ , F-DXR. Results are given as means  $\pm$  S.D.,  $n$ , 3.

Fig. 3 shows that when the CL-DXR was administered i.v., more DXR was taken up by the liver than that of F-DXR. Unlike the CL-DXR, when LRP-L-DXR was administered i.v., DXR taken up by the liver tissue was less than that of F-DXR. The AUC values of F-DXR, CL-DXR and LRP-L-DXR in the liver were 28.30, 37.92 and 26.51 (h  $\mu$ g/g), respectively (Table 2).

Fig. 4 shows that when LRP-L-DXR was administered i.v., DXR taken up by the spleen was more than that of F-DXR, but less than that of

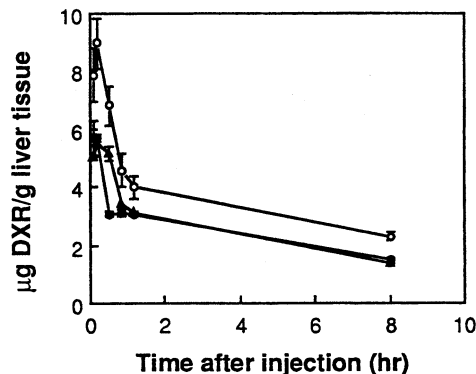


Fig. 3. Drug levels in liver tissue after i.v. injection of doxorubicin (DXR) of different formulations into C57BL/6 mice at a dose of 5 mg DXR/kg.  $\bullet$ , LRP-L-DXR;  $\circ$ , CL-DXR;  $\blacktriangle$ , F-DXR. Results are given as means  $\pm$  S.D.,  $n$ , 3.

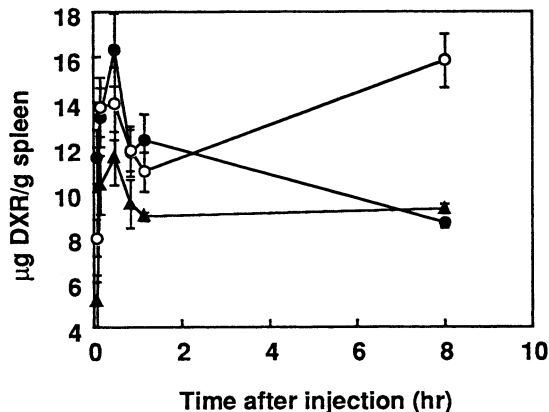


Fig. 4. Drug levels in spleen tissue after i.v. injection of doxorubicin (DXR) of different formulations into C57BL/6 mice at a dose of 5 mg DXR/kg.  $\bullet$ , LRP-L-DXR;  $\triangle$ , CL-DXR;  $\blacktriangle$ , F-DXR. Results are given as means  $\pm$  S.D.,  $n$ , 3.

CL-DXR. Fig. 5 shows that when LRP-L-DXR was administered i.v., DXR in the kidney was more than that of F-DXR and CL-DXR. Fig. 6 shows that the lung biodistributions of DXR of different formulations have no obvious difference among each other.

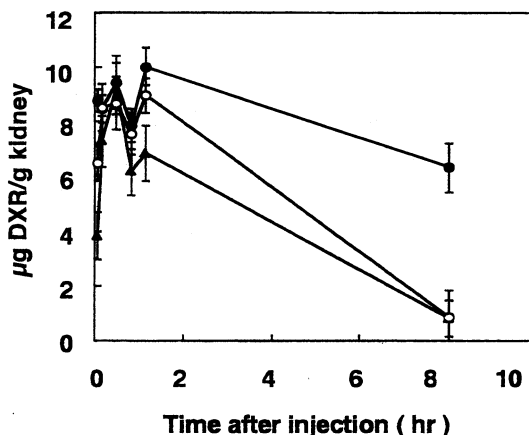


Fig. 5. Drug levels in kidney tissue after i.v. injection of doxorubicin (DXR) of different formulations into C57BL/6 mice at a dose of 5 mg DXR/kg.  $\bullet$ , LRP-L-DXR;  $\circ$ , CL-DXR;  $\triangle$ , F-DXR. Results are given as means  $\pm$  S.D.,  $n$ , 3.

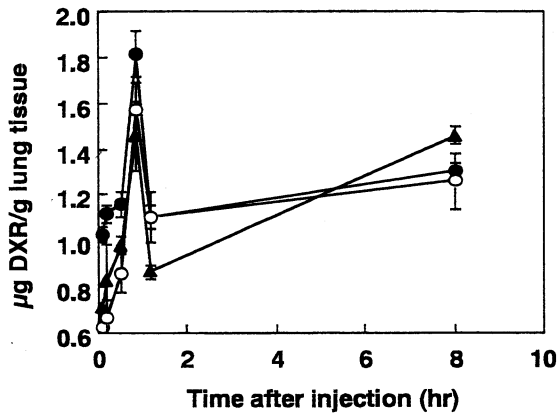


Fig. 6. Drug levels in lung tissue after i.v. injection of doxorubicin (DXR) of different formulations into C57BL/6 mice at a dose of 5 mg DXR/kg., ● LRP-L-DXR; ○, CL-DXR; ▲, F-DXR. Results are given as means  $\pm$  S.D.,  $n$ , 3.

### 3.3. Acute toxicity experiment

The death rates of the mice administered F-DXR and LRP-L-DXR in different doses are shown in Table 3. Table 3 shows that the maximum tolerance dose of LRP-L-DXR was close to 15.0 mg/kg and the maximum tolerance dose of F-DXR was close to 8.3 mg/kg.

### 3.4. Anticancer experiment

The comparison of the anticancer effects of LRP-L-DXR and F-DXR is shown in Table 4. Table 4 shows that in the ascitic M5076 tumor model, the anticancer effect of LRP-L-DXR was significantly increased compared with that of F-DXR. At the dose of 5.6 mg/kg, the ILS of F-DXR group was 34.9%; while the ILS of the LRP-L-DXR group was 64.6%. At the dose level of 8.3 mg/kg the ILS of F-DXR group was 39.8%;

Table 2

AUC<sup>a</sup> (h  $\mu$ g/g) of biodistribution curves of DXR of different formulations in heart, liver, spleen, lung and kidney

Formulations	Heart	Liver	Spleen	Lung	Kidney
F-DXR	36.05	28.30	75.66	9.47	53.69
CL-DXR	58.72	37.92	99.94	9.28	67.23
LRP-L-DXR	28.92	26.51	94.07	10.07	72.74

<sup>a</sup> AUC of heart,  $\sim$ 0–48 (h); AUC of the other tissues, 0–8 (h).

Table 3

Death rates of ascitic M5076 tumor-bearing C57 BL/6 mice within 10 days following iv. administration of F-DXR and LRP-L-DXR in different doses 5 days after inoculation

Dose (mg DXR/kg)	Death rates (%)	
	LRP-L-DXR	F-DXR
5.6	0	0
8.3	0	10
11.3	0	30
15.0	10	100
17.5	30	100

while the ILS of LRP-L-DXR group was 72.4%. At both doses, the ILS of the LRP-L-DXR group was significantly increased compared with that of the F-DXR group.

There was no significant difference between the anticancer effects of LRP-L-DXR and Doxil, as shown in Fig. 7.

## 4. Discussion

When LRP-L was mixed with saline containing DXR, liposomes form and automatically load DXR. The average diameter of LRP-L-DXR in saline was  $129.0 \pm 1.9$  nm and the encapsulation efficiency was  $98.1 \pm 0.6\%$ . The particle size distribution of the liposomes prepared with the conventional proliposome was 200–5000 nm and the encapsulation efficiency of water soluble drug was low. At present, in liposome technology, the particle size distribution is controlled by the extruder method and the encapsulation efficiency is increased using the ammonium sulfate gradient method. In LRP-L, oleic acid sodium salt and glycerin were used to decrease the particle size of

Table 4

Antitumor effect of F-DXR and LRP-L-DXR in the tumor model of ascitic M5076 in C57BL/6 mice

Agents	Dose of DXR (mg kg <sup>-1</sup> ) <sup>a</sup>	MST (days ± S.D.) <sup>b</sup>	ILS (%) <sup>c</sup>	Lethal toxicity (%)
Control	–	18.1 ± 0.7	–	0
F-DXR	5.6	24.6 ± 0.9	34.9	0
	8.3	25.3 ± 0.9*	39.8	10
LRP-L-DXR	5.6	29.8 ± 2.8	64.6**	0
	8.3	31.2 ± 1.4	72.4***	0

<sup>a</sup> Single i.v. starting 5 days after inoculation through the tail vein of the mice.

<sup>b</sup> Mean survival time of mice of each group.

<sup>c</sup> Increase of life span of each group.

\* One animal died within 10 days and not included in the calculation.

\*\*  $P < 0.001$ , compared with F-DXR (5.6 mg DXR/kg).

\*\*\*  $P < 0.001$ , compared with F-DXR (8.3 mg DXR/kg).

the liposomes and increase the encapsulation efficiency. Oleic acid sodium salt was inlaid into the membranes of the liposomes to increase the negative zeta potential of liposomes and therefore the liposomes could automatically load positively charged DXR, which was a novel kind of remote-loading technology and much easier than the conventional remote loading technologies, such as the ammonium sulfate gradient method used in Doxil (Working et al., 1994). To increase the circulation time of LRP-L-DXR in the blood circulating system, PEG-DSPE was attached to the membrane of the liposomes, which was almost the same as the reported long circulation technology (Working et al., 1994). In addition, LRP-L was different from the conventional proliposome that was composed of crystal powders covered by lipid bimolecular membrane (Katare et al., 1991a).

The findings of the pharmacokinetics indicate that the clearance of LRP-L-DXR from plasma was 22 and five times those of F-DXR and CL-DXR, respectively. Therefore, LRP-L-DXR circulated for a longer time in the blood stream following i.v. administration, which could result in more LRP-L-DXR accumulating in the cancer tissue and increase the anticancer effect of DXR.

The findings of the biodistribution experiment indicate that when injected into the blood stream, LRP-L-DXR in the heart tissue was less than that of CL-DXR and not more than that of F-DXR. The findings of LRP-L-DXR biodistribution in the heart were also different from that reported of

Doxil which was more than that of F-DXR following i.v. administration (Working et al., 1994). Since the heart was full of blood and the blood concentration of CL-DXR or LRP-L-DXR was higher than that of F-DXR, the biodistribution data of CL-DXR and LRP-L-DXR could not exactly reflect the biodistribution of CL-DXR and LRP-L-DXR in the heart. However, the data indicate that LRP-L-DXR taken by the heart tissue was less than that of F-DXR following i.v. administration. Since the CL-DXR was not protected by PEG-DSPE, 24 h later, the CL-DXR

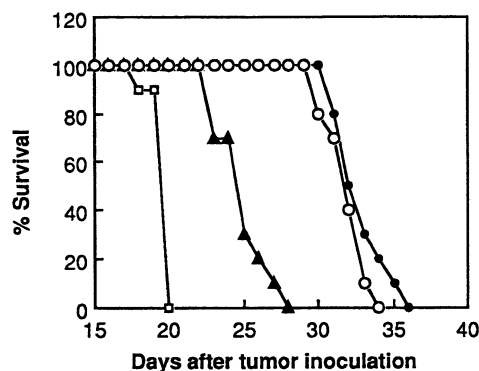


Fig. 7. Therapeutic efficacy of LRP-L-DXR and Doxil in the ascitic M5076 tumor model. C57BL/6 mice were inoculated i.p. with  $10^6$  M5076 carcinoma cells and treated 5 days later with 8.3 mg/kg F-DXR, LRP-L-DXR or Doxil administered i.v. The number of mice in each group was 10. There was no significant difference between the anticancer effects of LRP-L-DXR and Doxil ( $P > 0.05$ ). ●, Doxil; ○, LRP-L-DXR; ▲, F-DXR; □, Untreated.

could be destroyed by MPS in the liver and part of DXR was released, which might result in more DXR accumulating in the heart tissue compared with that of F-DXR and LRP-L-DXR (Fig. 2). LRP-L-DXR was protected by PEG-DSPE and was more stable while circulating in the blood stream than F-DXR and CL-DXR. Therefore, DXR was released more slowly from the LRP-L-DXR depot. This explanation was supported by the comparison of the liver biodistribution of DXR of different formulations.

Unlike that of CL-DXR, when injected into the blood stream, the biodistribution of LRP-L-DXR in the liver tissue was not more than that of F-DXR because of the protective action of PEG-DSPE (Fig. 3), which was also different from the reported result of Doxil which was more than that of F-DXR (Working et al., 1994). However, the biodistribution of LRP-L-DXR in the spleen was less than that of CL-DXR but more than that of F-DXR (Table 2 and Fig. 4), which was similar to the reported result of Doxil (Working et al., 1994). Therefore, LRP-L-DXR was destroyed by the liver more slowly than CL-DXR and F-DXR, while DXR was released from LRP-L-DXR more slowly. These explanations were also supported by the comparison of the kidney biodistribution of DXR of different formulations (Fig. 5). Since less LRP-L-DXR was taken up by the liver tissue, more LRP-L-DXR was detected in the kidney, which was similar to that of Doxil (Working et al., 1994).

Toxicity and therapeutic experiments indicate that the acute toxicity of LRP-L-DXR was significantly decreased and the anticancer effect was significantly increased compared with those of F-DXR. There was no significant difference between the anticancer effects of LRP-L-DXR and Doxil. The mechanism responsible for the increased therapeutic effects and reduced toxic responses of DXR involves a variety of factors. It is believed that the increased permeability of tumor vasculature is the main factor which results in the accumulation of liposomal anticancer agents into the tumor tissue (Wu et al., 1993; Vaage et al., 1997). However, the long-circulation appears not to be the only factor responsible for the increase of anticancer effect of LRP-L-DXR. The pharma-

cokinetic experiment indicates that the clearance of CL-DXR was less than 1/4 that of F-DXR and the AUC was greater than 4-fold that of F-DXR, which was also reported by other authors (Rahman et al., 1986a). However, the anticancer effect of CL-DXR was not increased compared with that of F-DXR (data was not shown), which was also reported by other authors (Rahman et al., 1986b). This suggests that since LRP-L-DXR is protected by PEG-DSPE against the destruction of MPS, LRP-L-DXR forms a bigger depot of DXR in vivo compared with those of F-DXR and CL-DXR (without protection) and, therefore, greater quantities of free DXR will be released more slowly from the depot and accumulate in cancer tissue to kill cancer cells.

In conclusion, following i.v. injection, the plasma concentration–time curve of LRP-L-DXR was best fitted to a triexponential decay curve and circulated for a longer period than those of F-DXR and CL-DXR, which was realized mainly through the inhibition of the uptake of the LRP-L-DXR by the liver. The toxicity of LRP-L-DXR was significantly decreased and its anticancer effect was significantly increased compared with those of F-DXR. There was no significant difference between the anticancer effects of LRP-L-DXR and Doxil in the ascitic M5076 tumor model of C57BL/6 mice. Unlike Doxil, in the preparation of LRP-L-DXR, the ammonium sulfate gradient method and the extruders were not used. In addition, the LRP-L can be used to carry other positive charged anticancer agents, which needs further research.

## Acknowledgements

This work was supported by grants from FIP the Nagai Foundation Tokyo and the Ministry of Education, Science, Sports, and Culture, Japan.

## References

- Batzri, S., Korn, E.D., 1973. Single bilayer liposomes prepared without sonication. *Biochim. Biophys. Acta* 298, 1015–1019.



- Cox, S.K., Wilke, A.V., Frazier, D., 1991. Determination of adrimycin in plasma and tissue biopsies. *J. Chromatogr.* 564 (1), 322–329.
- Fossen, E.A., Tokes, Z.A., 1979. In vitro and in vivo studies with adrimycin liposomes. *Biochem. Biophys. Res. Commun.* 91 (4), 1295.
- Lee, H.J., Ahn, B., Paik, W.H., Shim, C., Lee, M.J., 1996. Inverse targeting of reticuloendothelial system-rich organs after intravenous administration of adriamycin-loaded neutral proliposomes containing poloxamer 407 to rats. *Int. J. Pharm.* 131, 91–96.
- Paney, N.I., Browning, I., Hynes, C.A., 1986a. Characterization of proliposome. *J. Pharm. Sci.* 75, 330–333.
- Paney, N.I., Timmis, P., Ambrose, C.V., Warel, M.D., Ridway, F., 1986b. Proliposomes: a novel solution to an old problem. *J. Pharm. Sci.* 75, 325–329.
- Katara, O.P., Vyas, S.P., Dixit, V.K., 1991a. Proliposomes on indomethacin for oral administration. *J. Microencap.* 8, 295–300.
- Katara, O.P., Vyas, S.P., Dixit, V.K., 1991b. Preparation and performance evaluation of pain proliposomal systems for cytoprotections. *J. Microencap.* 8, 295–300.
- Rahman, A., Carmichael, D., Harris, M., Rohr, J.K., 1986a. Comparative Pharmacokinetics of free doxorubicin entrapped in cardiolipin liposomes. *Cancer Res.* 46, 2295–2299.
- Rahman, A., Fumagalli, A., Barbieri, B., Schein, P.S., Casazza, A.M., 1986b. Antitumor and toxicity evaluation of free doxorubicin and doxorubicin entrapped in cardiolipin liposomes. *Cancer Chemother. Pharmacol.* 16 (1), 22–27.
- Rahman, A., White, G., more, N., Schein, P.S., 1985. Pharmacological, toxicological and therapeutic evaluation in mice of doxorubicin entrapped in cardiolipin liposomes. *Cancer Res.* 44, 5427–5432.
- Vaage, J., Donovan, D., Uster, P., Working, P., 1997. Tumor uptake of doxorubicin in polyethylene-glyco coated liposomes and therapeutic effect against xenografted human pancreatic carcinoma. *Br. J. Cancer* 75, 482–488.
- Wang, J.P., Su, D.S., Gu, X.Q., 1994. Studies on adriamycin proliposome prepared by spray drying method. *Chinese Pharm. J.* 3, 149–151.
- Working, P.K., Newman, M.S., Huang, S.K., et al., 1994. Pharmacokinetics, biodistribution and therapeutic efficacy of doxorubicin encapsulated in Stealth® liposomes (Doxil®). *J. Liposome Res.* 4, 667–687.
- Wu, N.Z., Da, D., Ruddoll, T.L., Needham, D., Whorton, R., Dewhirst, M.W., 1993. Increased microvascular permeability contributes to preferential accumulation of STEALTH liposomes in tumor tissue. *Cancer Res.* 53, 3765–3770.
- Yamaoka, K., Tanigawara, Y., Nakagawa, T., Uno, T., 1981. A pharmacokinetic analysis program (multi) for microcomputer. *J. Pharmacobiodyn.* 4 (11), 879–885.